

Air Force Institute of Technology

AFIT Scholar

Faculty Publications

11-27-2006

Multi-port Beam Combination and Cleanup in Large Multimode Fiber Using Stimulated Raman Scattering

Brian M. Flusche

Thomas G. Alley

Timothy H. Russell

Won B. Roh

Follow this and additional works at: <https://scholar.afit.edu/facpub>



Part of the [Plasma and Beam Physics Commons](#)

Multi-port beam combination and cleanup in large multimode fiber using stimulated Raman scattering

Brian M. Flusche^{1,2}, Thomas G. Alley¹, Timothy H. Russell¹, and Won B. Roh^{1,3}

¹Department of Engineering Physics, Air Force Institute of Technology, 2950 Hobson Way, AFIT/ENP, Wright-Patterson Air Force Base, Ohio 45433, USA

²Department of Physics, 2354 Fairchild Drive, Suite 2A85, US Air Force Academy, CO, 80840, USA

³Deceased

thomas.alley@afit.edu

Abstract: We demonstrated the successful combination and cleanup of four laser beams via stimulated Raman scattering (SRS) using a multi-port fiber combiner and a large multimode fiber. Multiple Stokes orders were observed in the output, but loss at longer wavelengths reduced the transmission of the higher Stokes orders and limited the SRS conversion efficiency. SRS beam cleanup was also investigated using a single laser beam. The output beam had a measured M^2 better than 2 for fiber lengths from 400-1400 meters.

© 2006 Optical Society of America

OCIS codes: (190.4370) Nonlinear optics, fibers; (190.5650) Raman effect; (190.5890) Scattering, stimulated

References and links

1. H. J. Eichler, A. Haase and O. Mehl, in *High Power Lasers—Science and Engineering*, R. Kossowsky, M. Jelinek, and R. F. Walter, eds. (Kluwer Academic Publishers, Boston, 1996), p. 241.
2. T. Y. Fan, "Laser Beam Combining for High-Power, High-Radiance Sources," *IEEE J. Sel. Top. Quantum Electron.* **11**, 567-577 (2005).
3. K. S. Chiang, "Stimulated Raman scattering in a multimode optical fiber: evolution of modes in Stokes waves," *Opt. Lett.* **17**, 352-354 (1992).
4. J. T. Murray, W. L. Austin, and R. C. Powell, "Intracavity Raman conversion and Raman beam cleanup," *Opt. Mater.* **11**, 353-371 (1999).
5. T. H. Russell, S. M. Willis, M. B. Crookston, and W. B. Roh, "Stimulated Raman scattering in multimode fibers and its application to beam cleanup and combining," *J. Nonlinear Opt. Phys. Mater.* **11**, 303-316 (2002).
6. S. H. Baek, and W. B. Roh, "Single-mode Raman fiber laser based on a multimode fiber," *Opt. Lett.* **29**, 153-155 (2004).
7. C. A. Codemard, P. Dupriez, Y. Jeong, J. K. Sahu, M. Ibsen, and J. Nilsson, "High-power continuous-wave cladding-pumped Raman fiber laser," *Opt. Lett.* **31**, 2290-2292 (2006).
8. G. P. Agrawal, *Nonlinear Fiber Optics* (Academic Press, New York, 2001).
9. L. Lombard, A. Brignon, J. P. Huignard, E. Lallier and P. Georges, "Beam cleanup in a self-aligned gradient-index Brillouin cavity for high-power multimode fiber amplifiers," *Opt. Lett.* **31**, 158-160 (2006).

1. Introduction

High-Power solid-state lasers often suffer from thermally induced aberrations [1] which are detrimental to applications that rely on laser brightness. Recent investigations [2] in beam combining have sought to combine semiconductor laser arrays, solid state lasers and fiber lasers with both coherent methods and spectral methods to achieve good output beam quality. Some methods use active electronic control to coherently phase an array while others use passive optical techniques that can produce either coherent output or spectrally broad output. In this paper a method is investigated that can convert an aberrated input beam into a good quality output or passively combine several lasers into a single good quality beam with many

spectral orders in the output. The method relies on the intrinsic beam cleanup properties of stimulated Raman scattering in a graded-index multimode fiber which produces preferential gain in the fundamental mode [3-7].

Using this approach, we demonstrated for the first time that four pulsed laser beams can be combined into a single good quality beam. The output from each laser was focused into one channel of a squid-like fiber beam combiner consisting of many inputs and one much larger output. This physical arrangement overlaps the beams spatially, but because of conservation of etendue, the beam quality does not improve over that of the input. The resulting beam is then directed into a long fiber which can be cleaned up through stimulated Raman scattering (SRS). The four pulsed laser beams were coherent with each other because they were split off from a single source. Four independent pulsed sources were not available, however we predict the Raman beam cleanup effect to occur regardless of whether the input is from a number of coherent sources or incoherent sources, as long as the threshold power condition is met for the specific Raman gain bandwidth [8]. This is based on our experience with similar work in stimulated Brillouin scattering [5].

Previous research has demonstrated beam cleanup of single input beams using SRS in fiber [3, 5], and two beam combination and beam cleanup through stimulated Brillouin scattering (SBS) [5, 9]. Because the Brillouin gain bandwidth is so small (~ 100 MHz), SBS beam combination or beam cleanup requires a narrow frequency pump which imposes a difficult constraint for high power solid state lasers. The larger Raman gain bandwidth (~ 40 THz) removes this pump restriction making the technique more attractive for many high power solid state lasers [8]. The previous research into SRS beam cleanup demonstrated its effectiveness in gradient index fiber with core diameters up to at least $50\ \mu\text{m}$ [5]. Combining multiple beams with a fiber combiner and SRS beam cleanup requires even larger multimode fiber with cores diameters equal to or greater than $100\ \mu\text{m}$ so that most of the light output from the fiber combiner can be collected in the multimode fiber. The utility of using large multimode fibers and the practicality of power scaling SRS beam cleanup in this geometry were explored.

2. Experimental setup

A schematic of the experimental setup is shown in Fig. 1. The source was a Q-switched Nd:YAG laser operating at 1.064 microns. The output was pulsed at 1.4 kHz and each pulse was ~ 100 nsec long. In order to demonstrate beam combination the beam was split into 4 unique paths. First, a polarization beam splitting (PBS) cube evenly split the energy of the pulses into two paths. Secondly, a 50/50 beam splitter followed in each leg providing four channels of roughly equal input energy.

Beam combination and cleanup was demonstrated in two separate spools of graded index (GI) germano-silicate fiber. One was 2.2 km long with a $100\ \mu\text{m}$ core and a numerical aperture (NA) of 0.29. The second spool was 2.5 km, had a $200\ \mu\text{m}$ core and a $\text{NA} = 0.275$. To demonstrate beam combination the four beams described above were coupled into four input channels of a multimode seven-port "squid"-like fiber beam combiner (FBC) shown in the inset of Fig. 1. Each input had a core diameter of $100\ \mu\text{m}$ ($\text{NA} = 0.19$). The output of the FBC had a core diameter of $105\ \mu\text{m}$ and an NA of 0.49. This experiment was meant as a conceptual demonstration, so the demonstration was made with fibers and FBC which we were not able to optimize to match. As a result of the mismatch in fiber diameter and numerical aperture, at best, only 32% of the energy exiting the FBC could be coupled into the $100\ \mu\text{m}$ fiber, while ideally, all of the output could be coupled into the $200\ \mu\text{m}$ fiber. It should be possible to avoid the loss caused by the mismatch and free-space launching of power into the fiber if one is able to fusion-splice matching FBC and fibers together.

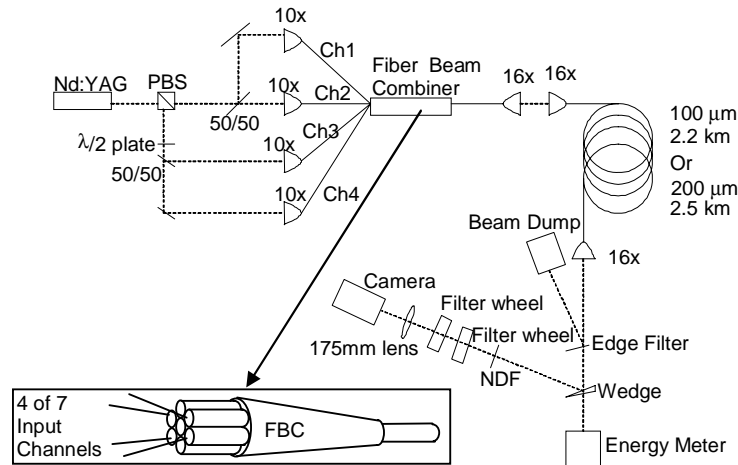


Fig. 1. Experimental setup to demonstrate four channel beam combination and cleanup.

The 16x microscope objectives after the FBC resulted in maximum coupling efficiency into the Raman active fiber. The edge filter at the output end of the fiber reflected any residual pump light into a beam dump, ensuring no pump light was present when diagnostics were performed. The wedge served as a pickoff, allowing diagnostics but preventing damage to sensitive equipment.

After all SRS measurements were performed, a one meter length was cut off the fiber spool, without changing the input alignment. The energy transmitted through this one meter segment was assumed to be the total power coupled into the fiber at each laser pump power setting. This enabled an accurate measurement of Stokes conversion efficiency in the fiber.

Figure 2 shows the experimental setup used to investigate the impact of fiber length on Stokes beam quality. The same laser source described above was used, but it was not split into four paths and was operated at 2 kHz. For this investigation, the fiber was cut to a series of different lengths, and the Stokes beam quality was measured for each fiber length. The 100 μm fiber was initially 1.3 km, but was shortened in 50 m or 100 m increments. For this experiment, beam quality was measured at both a constant diode pump current on the Nd:YAG laser and at a diode pump current that was two times above the Stokes threshold. The constant diode pump current ensured that the characteristics of the incoming pump laser were uniform throughout the test. However, as the fiber length was shortened, the SRS threshold energy increased. As a result, at a constant pump current, less and less energy was available to transfer to the Stokes beam. Additional data points were taken at two times above the Stokes threshold to ensure consistency in terms of the Stokes beam characteristics. Due to thermal effects, the Nd:YAG laser output power depended on both the diode pump current and the amount of warm-up time the laser was allowed. Because of this, the Stokes threshold was measured immediately before each beam quality measurement so that two times above threshold could be properly calculated.

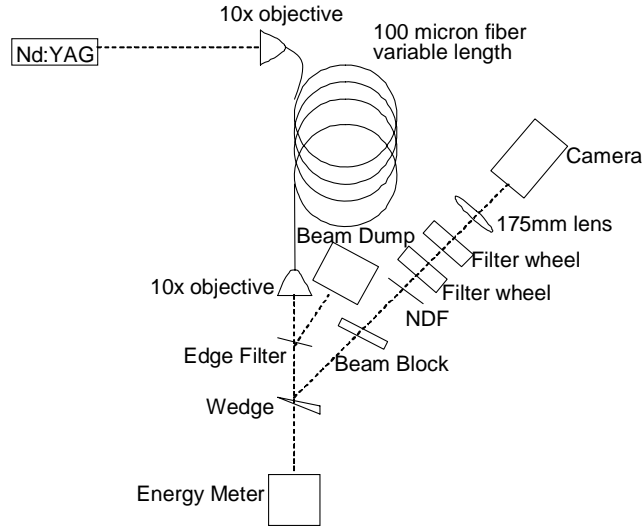


Fig. 2. Experimental setup for observing beam cleanup in 100 μm core size fiber.

3. Results and discussion

Beam combination was observed in both fibers pumped by the four-channel fiber squid. Figure 3 depicts the far-field images of all 4 transmitted pump beams (a) and (c) and of the combined Stokes beams (b) and (d) emerging from the rear fiber facet. Transmitted pump beam images were captured after cutting the fiber to a one meter length of fiber, indicating the input pump beam profile. The first two images (a) and (b) correspond to data collected from the 100 μm fiber, the last two images (c) and (d) correspond to the pump and Stokes transmitted through the 200 μm fiber. Each image depicts the same spatial extent, thus clearly the far-field spot of the Stokes beam is significantly smaller than that of the pump.

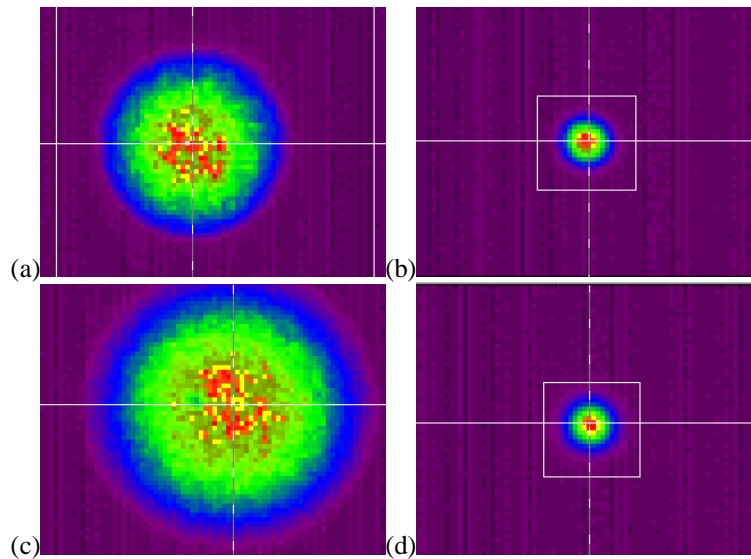


Fig. 3. Beam combination as demonstrated by pictures observed in the focal plane of a 175 mm lens of transmitted pump and generated Stokes beams from both 100 μm and 200 μm fibers. From top left: (a) 100 μm pump beam, $M^2 = 26.10$ (b) 100 μm Stokes beam, $M^2 = 2.64$ (c) 200 μm pump beam, $M^2 = 42.10$ (d) 200 μm Stokes beam, $M^2 = 2.75$

To quantify the improved spatial quality of the Stokes beam over that of the pump, the beam quality was measured in terms of M^2 . The pump transmitted through the 100 micron fiber had a measured beam quality of $M^2 = 26.1$. The corresponding Stokes beam was measured to be $M^2 = 2.6$. The 200 micron fiber supported more modes resulting in a pump beam quality of $M^2 = 42.1$, but it still yielded a relatively good Stokes beam corresponding to the combined contribution from the 4 pump beams, $M^2 = 2.8$.

In addition to beam quality, the beam combination performance was also characterized by the efficiency of pump beams exciting a Stokes output. The conversion efficiency was measured relative to the amount of power coupled into the fiber and is shown for a variety of pump powers in Fig. 4.

A comparison of the maximum efficiency for the two fibers indicates that the 100 micron fiber is preferable due to its lower threshold, but considering the significant coupling losses for the 100 micron fiber (described above to be 31% at best), the 200 micron fiber has a better overall conversion at its peak. In both curves, as the pump energy was increased beyond the maximum efficiency, the measured Stokes conversion went down. The decrease in efficiency was due to more energy forced into higher Stokes orders with increasing pump energy. The higher Stokes orders were in turn attenuated at a much higher rate than the first order due to the larger loss of longer wavelengths in glass. Because of this power loss to absorption, brightness conversion efficiency was not quantified, only beam quality.

The cascade of power to these longer wavelengths has been attributed to the combined effects of nondegenerate collinear four-wave-mixing and SRS [5]. The presence of the higher order Stokes modes was confirmed with a spectrum analyzer. The Stokes spectrum was evaluated at four different pulse energies. The spectrum analyzer data showed that at high pump energies, the transmitted pump and Stokes energy in each order was nearly steady despite any increase in pump energy. The results indicate that extra pump energy was converted to longer wavelengths and absorbed by the fiber. The spectral data for the 100 μm fiber are shown in Fig. 5 below, with the 200 μm fiber performing similarly.

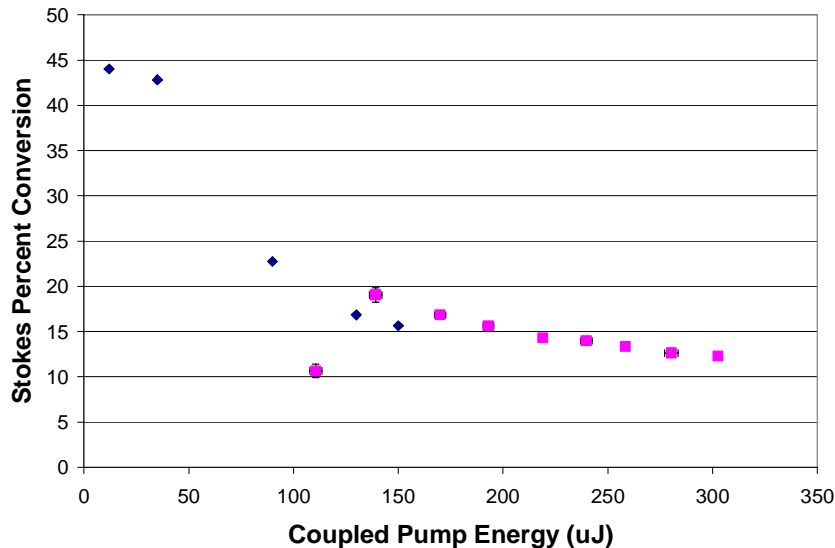


Fig. 4. Stokes percent conversion as a function of coupled pump energy for 100 μm fiber (diamonds) and 200 μm fiber (squares).

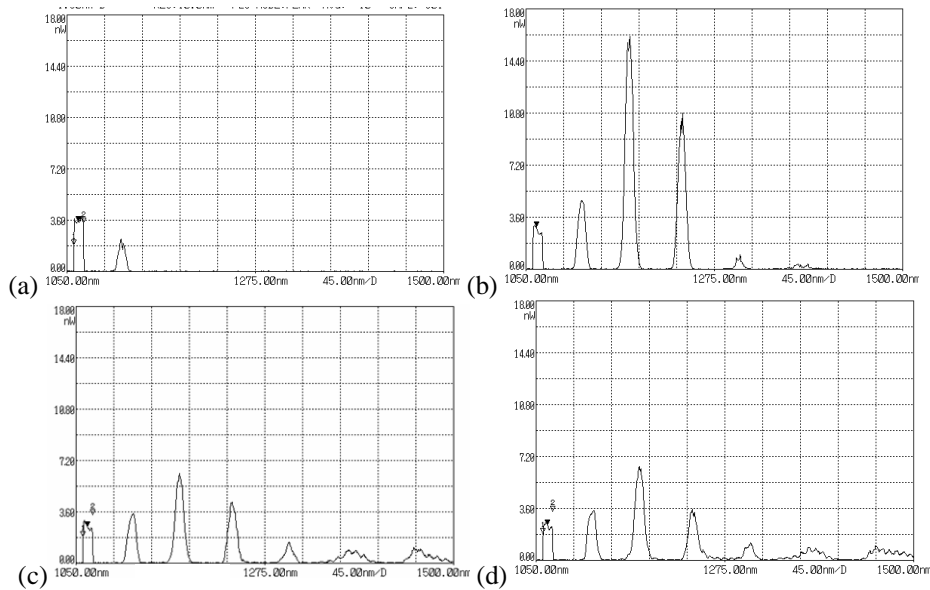


Fig. 5. Spectrum analyzer sweeps from 1050 nm to 1500 nm demonstrating fiber attenuation of higher Stokes orders. For all graphs, wavelength is displayed on the horizontal axis, while the vertical axis is a relative intensity measurement. (a) At 25 μJ per pulse, the Stokes threshold has been reached. The pump beam is shown at 1064 nm and the 1st order Stokes beam is present at 1116.5 nm. (b) At 35 μJ per pulse, the effects of four-wave mixing become apparent, with three well defined Stokes orders, and hints of a fourth and fifth order. (c) At 90 μJ per pulse, the higher attenuation of the fiber at longer wavelengths is shown, as the fifth and sixth Stokes orders are generated, but remain very low in intensity. (d) At 150 μJ per pulse, the relative intensities of the higher Stokes orders are almost unchanged from the sweep shown in (c).

Figure 6 demonstrates the Stokes output from all orders as a function of the power in the four input beams. The results of this analysis demonstrate a clear roll off in slope efficiency which we attribute to long wavelength absorption. Although the 100 μm fiber had a lower threshold, the 200 μm fiber produced more overall Stokes power at its maximum.

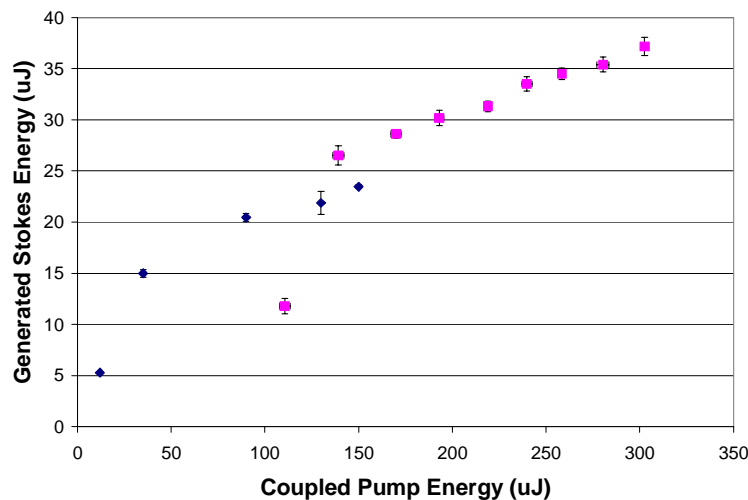


Fig. 6. Generated Stokes energy in 100 μm fiber (diamonds) and 200 μm fiber (squares) as a function of pump energy coupled into the fiber.

To characterize the dependence of Raman fiber beam cleanup on the fiber length, a 100 μm micron fiber was shortened in 50-100m increments. At each fiber length, two measurements of beam quality were performed: one at constant diode pump current and one at twice SRS threshold. Below 400 m, the effective length of the fiber was too short to achieve the Stokes threshold with the available pulse energy provided at the constant diode pump current. A graph of the beam quality results is shown in Fig. 7.

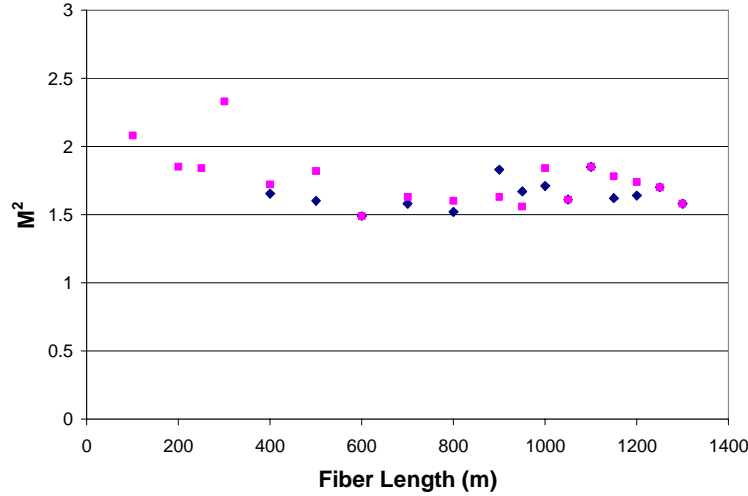


Fig. 7. M^2 value of the generated Stokes beam as a function of 100 μm core size fiber length. M^2 values were calculated for a diode pump current on the Nd:YAG pump laser of 12.9 A (diamonds) and two times above the Stokes threshold (squares).

As the figure demonstrates, for fiber lengths down to 400m, the beam quality of the Stokes output remains relatively constant between $M^2 = 1.5$ and $M^2 = 2$. The coupling of the pump beam was also held constant resulting in a coupled pump beam quality of $M^2 = 42$. Depending on the application, despite the increased threshold, it may be beneficial to use a shorter fiber to reduce the loss at the higher order Stokes wavelengths, thus increasing the overall output power. The exact reason for a relatively constant M^2 value of 1.5 to 2 is an open question that is currently being investigated. Although it appears there is preferential gain in the fundamental mode, there is sufficient gain in other low order modes to not completely achieve diffraction limited output. Far field pictures taken of the generated Stokes beam for various fiber lengths are shown in Fig. 8 below.

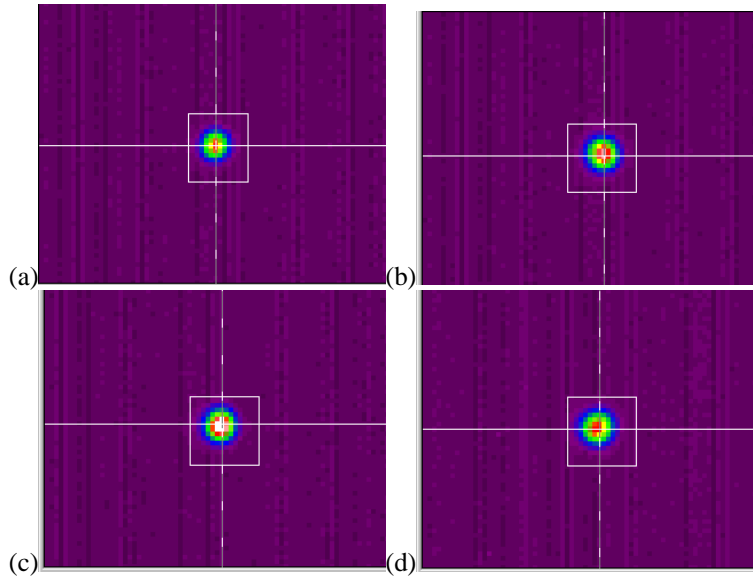


Fig. 8. Far field pictures of generated Stokes beam output from 100 μm fiber as a function of length. Pictures were all taken at a pump energy two times above the Stokes threshold. From top left: (a) 1300 m, $M^2 = 1.58$ (b) 1000 m, $M^2 = 1.84$ (c) 700 m, $M^2 = 1.60$ (d) 200 m, $M^2 = 1.85$.

4. Conclusion

We demonstrated successful four beam combination into a single beam with a cascade of spectral orders via a squid-like fiber beam combiner and SRS cleanup in 100 μm and 200 μm fibers. Large improvements in beam quality as measured by M^2 were observed. No significant change in M^2 of the generated Stokes beam was observed when fiber lengths greater than 400 m were used. Diminishing conversion efficiency in the SRS process used to clean up the beam was observed and likely results from absorptive loss in the fiber of the cascaded higher Stokes orders.

Acknowledgments

The authors thank the Air Force Research Laboratory (AFRL/DELO) for its partial support of this research.